Defect and Diffusion Forum
ISSN: 1662-9507, Vol. 452, pp 79-85
doi:10.4028/p-mYaQQ1

Submitted: 2025-09-28
Revised: 2025-12-23
Accepted: 2026-02-23
Online: 2026-05-18

Growth and Characterization of High-Quality Thick Epitaxial 4H-SiC Wafers for High Voltage Devices

Y. Li[1,a], J. Zhang[1,b], Z. Chen[1,c], H. Wang[1,d], K. Zhang[1,e], S. Hu[1,f], Raghothamachar[1,g], A. A. Burk Jr[2,h], K. Singh[2,i], M. A. Johar[2,j], N. A. Mahadik[3,k], R. E. Stahlbush[3,l], M. Dudley[1,m]

[1]Department of Materials Science & Chemical Engineering, Stony Brook University, Stony Brook, NY 11794 USA

[2]Coherent, Inc., USA

[3]U. S. Naval Research Laboratory, Washington DC, USA

[a]yuzhuo.li@stonybrook.edu, [b]jianpei.zhang@stonybrook.edu, [c]zeyu.chen@stonybrook.edu, [d]haochi.wang@stonybrook.edu, [e]kaixuan.zhang@stonybrook.edu, [f]shanshan.hu@stonybrook.edu, [g]balaji.raghothamachar@stonybrook.edu, [h]Albert.Burk@coherent.com, [i]kanwar.singh@coherent.com, [j]muhammadali.johar@coherent.com, [k]nadeem.mahadik@nrl.navy.mil, [l]stahlbush@nrl.navy.mil, [m]michael.dudley@stonybrook.edu

Keywords: Silicon Carbide, Thick Epitaxial Layer, X-ray Topography, 3C inclusions.

Abstract. Silicon carbide is a leading wide-bandgap semiconductor for high-voltage power electronics. For 6.5–10 kV operation, thick epitaxial layers (≥60 μm) are required to sustain depletion width and maintain uniform electric fields, placing a premium on low extended-defect densities in both substrate and epilayer. Thick epitaxial 4H-SiC layers of 60 μm and 110 μm were grown on 6-inch substrates in a multi-wafer warm-wall reactor and evaluated by synchrotron X-ray topography in grazing-incidence (22-4 16) and transmission (11-20) geometries. Transmission imaging showed substrate dislocation content near the lower bound typically reported for 6-inch wafers. Notably, grazing-incidence topography (penetration depth >40 μm) revealed no basal-plane dislocations propagating into the epilayers, consistent with efficient dislocation conversion at the substrate–epilayer interface. The 3C-SiC inclusion density was ~30 per 6-inch wafer for 60 μm epilayers and ~60 per wafer for 110 μm epilayers; the average micropipes density varies from 0 to 5 for both 60 and 110 um epiwafers. Threading dislocation densities—screw, edge, and mixed—were on the order of 1.0–2.0 × 10^3 cm^{-2}.
These results establish thick 4H-SiC epilayers with suppressed basal-plane propagation and substantially reduced extended-defect content, providing a strong basis for reliable 6.5–10 kV device fabrication.

Introduction

Silicon carbide (4H-SiC) has emerged as a central wide-bandgap semiconductor for high-voltage power conversion because its large bandgap, high thermal conductivity, and high critical electric field enable compact drift regions that sustain high blocking voltages with low conduction loss. In the 6.5–10 kV class (e.g., planar MOSFETs and superjunction devices), thick and uniform drift layers (typically ≥ 60 μm) are required to provide sufficient depletion width and a near-uniform electric-field distribution at breakdown, placing stringent demands on wafer-scale crystalline quality across both substrate and epitaxial layer [1,2].
Extended defects that are most consequential in this regime include basal-plane dislocations (BPDs), threading dislocations (screw/edge/mixed) (TSDs/TEDs/TMDs), micropipes, and 3C inclusions. For device reliability, a key objective in thick epitaxy is to suppress basal-plane-related degradation pathways, minimize threading dislocation densities to the low 10^3 cm^{-2} level across full 150 mm wafers, and eliminate high-leakage defects such as micropipes. [3-5]
Assessing these defect populations at the wafer scale with depth sensitivity is enabled by synchrotron X-ray topography (XRT). In off-axis 4H-SiC, grazing-incidence monochromatic topography

provides selective sensitivity to defects within the effective penetration depth near the surface—particularly for basal plane related defects and transmission geometries provide defect information primarily in the substrates.
In this work, thick epitaxial 4H-SiC layers of 60 μm and 110 μm were grown on 6-inch substrates using a multi-wafer warm-wall reactor and characterized by synchrotron XRT in complementary grazing-incidence (g = 22-416) and transmission (g = 11-20) geometries.

Experiment

4° off-axis PVT-grown 150 mm 4H-SiC wafers with 60 and 110 μm-thick CVD epilayers were characterized using synchrotron monochromatic beam X-ray topography (SMBXT) in grazing-incidence geometry with the 22-4 16 reflection at 18 keV, performed at beamline 1-BM of the Advanced Photon Source (APS), Argonne National Laboratory (experimental setup in Fig. 1a; Images were recorded on high-resolution X-ray films (Agfa D3sc). High-resolution X-ray diffraction (HRXRD) double- and triple-axis rocking curves and reciprocal-space maps (RSMs) of (0008) were measured on a Bede D1 diffractometer using Cu $K\alpha_1$ (λ=1.54 A). Figure 1(c) shows the double-axis geometry for rocking curve measurement. The laboratory source operated at 40 kV/30 mA; the beam was conditioned by a MaxFlux multilayer mirror and a channel-cut symmetric Ge(004) monochromator. [6]

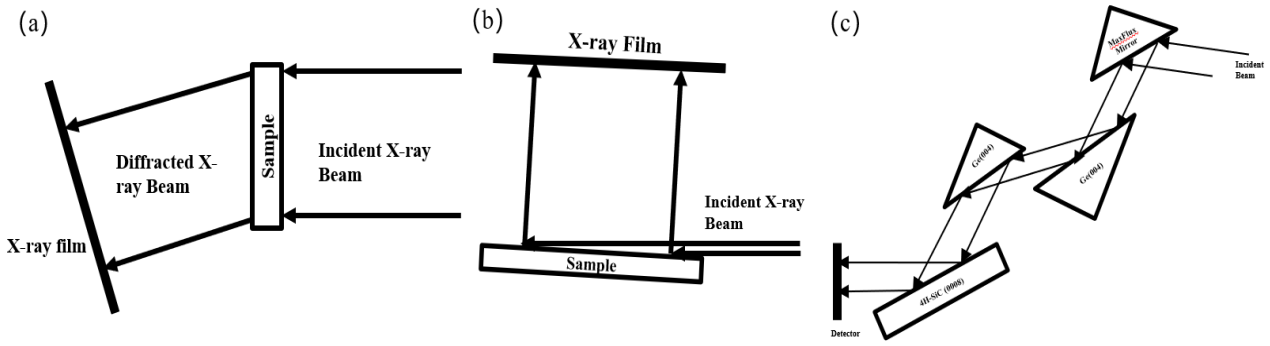

Fig. 1. Schematic of experiment setup of (a) Synchrotron x-ray topography with transmission geometry, (b) Grazing incidence geometry, (c) High resolution x-ray diffraction with double-axis and triple-axis scanning of (0008) reflection.

Results and Discussion

Grazing-incidence synchrotron X-ray topographs using the g = $22\bar{4}$ 16 reflection as an effective penetration depth of about 45 μm, imaging the 60 μm and 110 μm thickness epi layer 4H-SiC wafers. The HRXRD was used as an effective tool to reveal the general quality of the thick epi layer SiC wafers.
Overall wafer quality analysis. Fig. 2 shows transmission and grazing incidence topographs from 60um and 110um thick epiwafers. For 60 um epi layer wafers, the grazing topographs exhibit few broad contours and for 110 um epi layer wafers which show greater number and narrower contours, indicating a higher lattice distortion level than 60 um epi layer wafers. The double-axis rocking curve of these wafers given by HRXRD also confirm these observations withs: the average FWHM of 60 um epi layer wafers is 11 arcsec while that of the 110 um epilayer wafers is 13 arcsec, which correlates with the higher lattice distortion observed on the grazing incidence topographs. For these thick epilayer wafers, the number of 3C inclusion (except the edge of the wafer) incidence is of the order of tens per wafer (20 per 150 mm wafer for 60 μm; ≈ 50 per wafer for 110 μm). Few micropipes (1 or 2) were detected throughout the wafers, including in the 110 μm epilayers. The threading dislocation (TSD/TMD and TED) densities are relatively low for both thickness epi-wafers. The transmission topography (g= 11-20) indicates the dense BPDs from the substrate and relatively low TED densities (under 100 cm^{-2}). In grazing-incidence (22-4 16, 18 keV; ≈ 40 μm effective depth), no

BPD is observed within the epilayers except for localized features surrounding the 3C inclusions and the average TED density in grazing topography is 400 cm^{-2} for 60 μm epi layer and 500 cm^{-2} for 110 μm epi layer).

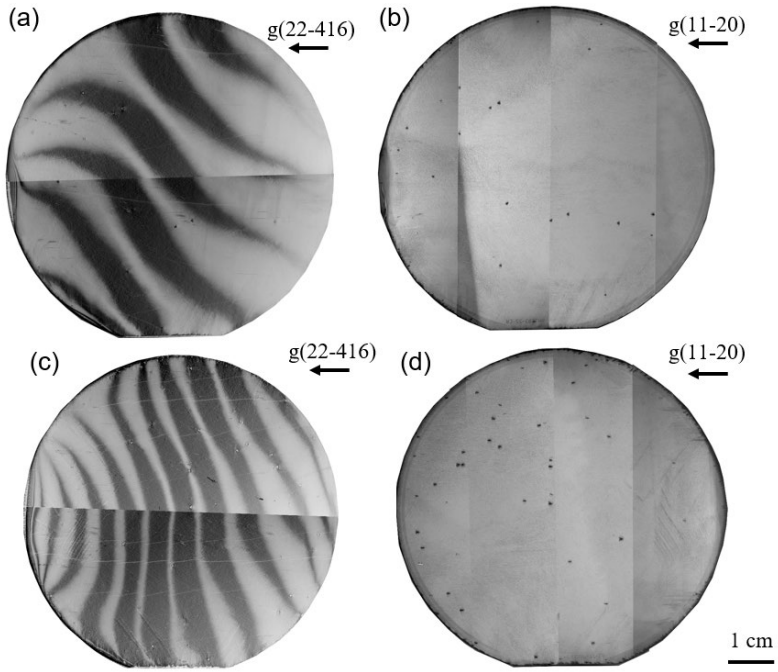

Fig. 2. Synchrotron X-ray topography of a 6-inch diameter 4H-SiC wafer with a 110 μm epitaxial layer: (a) Grazing-incidence topography (g = 22-416) of 60 um epi layer wafer and (c) 110 um epi layer wafer, highlighting surface and near-surface defect distributions and revealing 3C-SiC inclusions as distinct white contrast features; (b) Transmission topography (g = 11-20), providing comprehensive defect visualization of defects in substrate through the epitaxial layer depth, where 3C-SiC inclusions appear as characteristic black contrast features.

3C Inclusions, HLA, and ID. Overall, the 3C inclusions are few and occur mainly near the wafer edge; the interiors are largely inclusion-free. The enlarged grazing topographs (g=22-4 16) show the 3C inclusions with BPD loops generated. The BPD will propagate along <1-100> directions. The average width of 3C inclusions in 60 μm-thick epi layer wafers is about 860 μm. BPD loops and Interfacial dislocations are generated around the 3C inclusions. The average length of BPD propagation along <1-100> is 1000 um. The 3C inclusions and associated BPDs covered is about 0.5% throughout the wafer. In 110 μm-thick epilayer wafers, the average width of 3C inclusions is approximately 1500 μm, with BPD loops and interfacial dislocations forming around them. The basal-plane dislocations propagate along the <1-100> direction with the average length of about 1400 μm; the coverage of 3C inclusions and associated BPD loops over the wafer is 1.7%. Interfacial dislocations are observed in some 3C inclusions in both 60um and 110um epi layer wafers; the half-loop arrays, however, is not observed on these wafers.

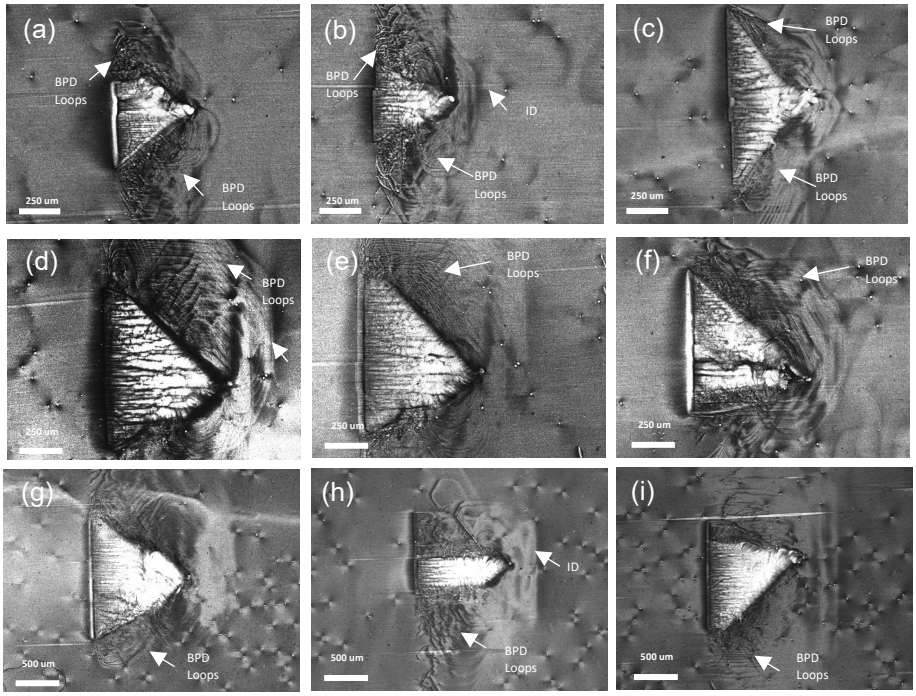

Fig. 3. Topographs of 3C inclusions from: (a) to (c) 40um epi layer wafers; (d) to (f) 60 um epi layer wafers; (g) to (i) 110 um epi layer wafers.

BPD Conversions. During the epitaxial growth of 4H-SiC on off-axis substrates, defects can be either replicated from the substrate into the grown epi layer or converted into other kinds of defects. One of the most important conversions is the BPD converting to TED. BPDs significantly affect SiC crystal quality and device reliability, leading to issues such as forward-voltage degradation in SiC p–n diodes under long-term operation [7] and increased leakage current. The BPD conversion in the epi layer growth, therefore, is critical to decrease the BPDs in the epi layer. BPDs originating in the substrate intersect the stepped growth surface. Because the surface advances in step-flow mode, the dislocations interact with terraces and macro-steps. As the BPD approaches the surface, it experiences an image force arising from the nearby free surface; this force becomes comparable to the critical resolved shear stress for prism-plane glide. To minimize line energy, the BPD bends upward and out of the basal plane within the first few microns of epilayer growth. Once bent, the dislocation reorients and propagates vertically as a TED. Consequently, BPD density drops sharply while TED density rises across the interface. [8] [9].

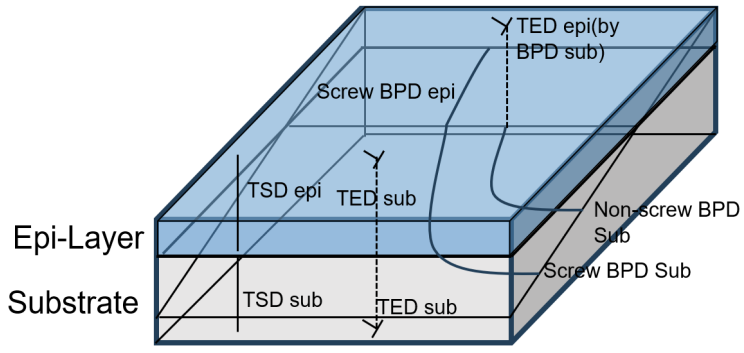

Fig. 4. Schematic of different kinds of defect movements during the epitaxial growth.

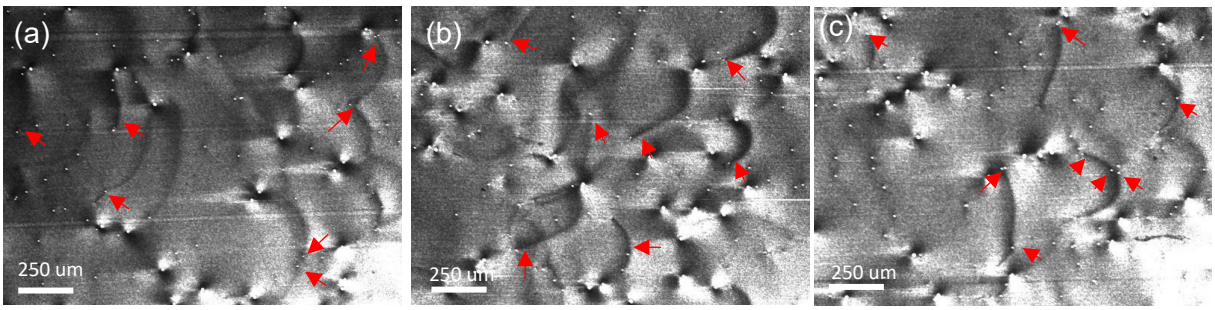

Fig. 5. Topographs with (22-4 16) under high magnitude optical microscopy of the thick epi layer wafers. The red arrows show the TEDs (white dot contrast) along with BPD (black line contrast), indicating the examples of BPD conversions during the epitaxial growth.

"**Zebra" feature defects in 60 µm Epi-Layer.** A prominent "zebra" band is observed in the 60 µm 4H-SiC epilayer wafer. Transmission synchrotron topography reveals a region of BPDs forming a large strain-contour loop, while grazing-incidence topography of the same region shows dense TEDs but no BPDs, confirming BPD to TED conversion within the epilayer. The persistence of the zebra-shaped contrast indicates that although the defect character has changed, the associated long-range strain/tilt field from substrate defect clusters has been elastically transferred into the epilayer. Previously, Liao et al. [10] reported butterfly defects, which originate from tightly bundled, oppositely signed BPDs forming lobes of tilt. The zebra shape defect observed differs in geometry, presenting instead as a large, loop-like strain field, whereas in the zebra shape defect, the entire defect region in transmission images is filled with dense BPDs, producing a much broader strain loop. Moreover, no well-defined LAGB nucleation site is observed for the zebra feature. However, the butterfly-type distortion field may represent a contributing condition, influencing the elastic strain environment that shapes the zebra band. Ongoing work is directed at clarifying this mechanism, disentangling the roles of substrate-induced dislocation clusters, macro-step overgrowth, and possible butterfly-like strain fields in the formation of this unique defect structure.

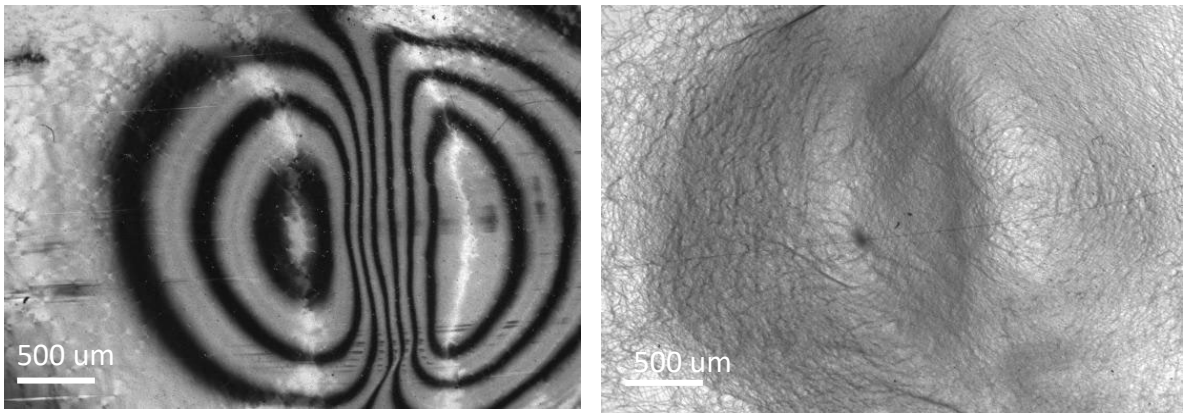

Fig. 6. Synchrotron X-ray topography of zebra feature defect of g= 22-4 16 grazing image (left) and g= 11-20 transmission image. The grazing image shows the black band contours with dense TEDs; the transmission image shows the dense BPD loop formed.

Scratches induced TED arrays. Scratch-induced TED arrays are observed in 40 µm and 110 µm thick epilayers, originating from residual scratches on the substrate surface that were not completely removed during polishing. Such scratches contain subsurface damage in the form of BPD half-loops, which act as dislocation sources during epitaxial growth. As growth proceeds, the intersections of these half-loops with the advancing surface replicate into the epilayer: intersections aligned in screw orientation propagate as screw-type BPDs, while those away from screw orientation propagate as TEDs. Because scratches usually extend laterally across the surface, many BPD loops intersect along the same trace, giving rise to rows of TEDs aligned with the scratch orientation. Synchrotron X-ray topographs show these arrays as closely spaced dislocations following the scratch line, often

appearing as opposite-signed pairs in accordance with Burgers vector conservation. With continued growth, these TED arrays can evolve in configuration, sometimes transforming into low-angle grain boundary-like structures further into the boule, though their density generally decreases with depth. [7,11]

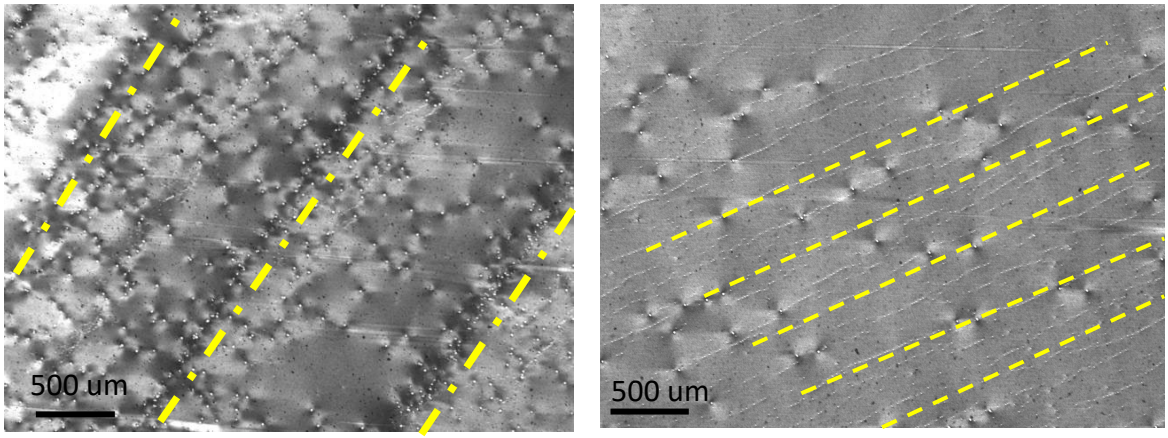

Fig. 7. Grazing incidence X-ray topography at high-magnification optical microscopy show scratches induced TED arrays in the 40 μm (left) epi layer wafer and in the 110 μm (right) epi layer wafer.

Summary

Synchrotron X-ray topography and high-resolution X-ray diffraction confirm the excellent crystalline quality of the thick 4H-SiC epilayers studied. Nearly complete BPD→TED conversion was achieved, while zebra-shaped bands and scratch-induced TED arrays provide insight into dislocation evolution. Grazing-incidence imaging shows no detectable BPD propagation into the epilayers except at 3C inclusions; 3C-SiC inclusions number about 30 per 6-inch wafer for 60-μm epilayers and ~50 for 110-μm epilayers. Only a few micropipes were observed, and threading dislocation densities were reduced to 200–400 cm^{-2}. These results underscore the significant potential of these wafers for reliable, high-performance power electronic devices.

Acknowledgements

This work has been funded, in part, by the Microelectronics Commons Program, a DOD initiative. The samples are provided by Coherent, Inc. This research used resources [or insert beamline if applicable] of the National Synchrotron Light Source II, a U.S. Department of Energy (DOE) Office of Science User Facility operated for the DOE Office of Science by Brookhaven National Laboratory under Contract No. DE-SC0012704. This research used resources of the Advanced Photon Source, a U.S. Department of Energy (DOE) Office of Science User Facility operated for the DOE Office of Science by Argonne National Laboratory under Contract No. DE-AC02-06CH11357. The Joint Photon Sciences Institute at SBU provided partial support for travel and subsistence for access to Advanced Photon Source.

References

[1] T. Kimoto, Material science and device physics in SiC technology for high-voltage power devices, Jpn. J. Appl. Phys. 54, 040103 (2015).

[2] Y. Zhang, H. Peng, Z. Chen, and M. Dudley, Investigation of factors influencing the occurrence of 3C-inclusions for the thick growth of on-axis C-face 4H-SiC epitaxial layers, J. Cryst. Growth 512, 1 (2019).

[3] K. Masumoto, K. Kojima, and H. Yamaguchi, Investigation of Factors Influencing the Occurrence of 3C-Inclusions for the Thick Growth of On-Axis C-Face 4H-SiC Epitaxial Layers, Materials 13, 4818 (2020).

[4] M. Dudley, N. Zhang, Y. Zhang, B. Raghothamachar, S. Y. Byrapa, G. Choi, E. Sanchez, D. M. Hansen, R. Drachev, and M. J. Loboda, Characterization of 100 mm diameter 4H-silicon carbide crystals with extremely low basal plane dislocation density, Mater. Sci. Forum 645–648, 291 (2010).

[5] B. Raghothamachar, M. Dudley, Dislocations in 4H-SiC Substrates and Epilayers, in: P. Wellmann, N. Ohtani, R. Rupp (Eds.), Wide Bandgap Semiconductors for Power Electronics, Wiley VCH GmbH, Weinheim, 2022, pp. 169-198.

[6] Z. Chen, Y. Liu, Q. Cheng, S. Hu, B. Raghothamachar, and M. Dudley, Analysis of strain in ion implanted 4H-SiC by fringes observed in synchrotron X-ray topography, J. Cryst. Growth 627, 127535 (2024).

[7] M. Dudley, N. Zhang, Y. Zhang, B. Raghothamachar, and E. K. Sanchez, Nucleation of c-axis screw dislocations at substrate surface damage during 4H-SiC homo-epitaxy, Mater. Sci. Forum 645–648, 295 (2010).

[8] S. Ha, P. Mieszkowski, M. Skowronski, and L. B. Rowland, Dislocation conversion in 4H silicon carbide epitaxy, J. Cryst. Growth 244, 257 (2002).

[9] H. Tsuchida, T. Miyanagi, I. Kamata, Y. Sugawara, et al., Investigation of basal plane dislocations in the 4H-SiC epilayers grown on {0001} substrates, Mater. Sci. Forum 483–485, 97 (2005).

[10] M.E. Liao, N. A. Mahadik, R. E. Stahlbush, A. Burk, U. Chakrabarti, I. Zwieback, X. Xu, and R. Rengarajan, Structural analysis of novel butterfly-shaped defects in 4H-SiC substrates, Proc. ICSCRM 2023 (2023).

[11] Q. Cheng, H. Peng, B. Raghothamachar, and M. Dudley, Scratch-induced threading dislocations in thick 4H-SiC epilayers, Defect Diffus. Forum 434, 71 (2024).